

CHARACTERISTICS OF A Mg-PALYGORSKITE IN MIOCENE ROCKS, MADRID BASIN (SPAIN)

E. GARCÍA-ROMERO^{1,*}, M. SUÁREZ BARRIOS² AND M. A. BUSTILLO REVUELTA³

¹ Departamento de Cristalografía y Mineralogía, Facultad de C. C. Geológicas, Universidad Complutense, Madrid, Spain

² Departamento de Geología, Universidad de Salamanca, Plaza de la Merced s/n 37008, Salamanca, Spain

³ Departamento de Geología, Museo Nacional de Ciencias Naturales, CSIC, José Gutiérrez Abascal 2, Madrid, Spain

Abstract—Palygorskite in Miocene mudstones, palustrine limestones and calcrites from the Esquivias locality (Madrid Basin, Spain) has been analyzed by X-ray diffraction, infrared spectroscopy, scanning electron microscopy, transmission electron microscopy and analytical electron microscopy to determine its characteristics and chemical composition. Other palygorskites from the literature are used as references. The mean structural formula obtained from the analysis of isolated particles is $(\text{Si}_{7.87}\text{Al}_{0.13})\text{O}_{20}(\text{Al}_{1.04}\text{Fe}^{3+}_{0.20}\text{Mg}_{3.11}\square_{0.65})(\text{OH})_2(\text{OH}_2)_4(\text{Ca}_{0.02}\text{K}_{0.05}\text{Na}_{0.08})$. This palygorskite has the largest Mg content reported in the literature, and it seems that, chemically, it fills the ‘compositional gap’ existing between sepiolite and palygorskite. Infrared spectroscopy reveals the absence of trioctahedral Mg and therefore the possibility of the existence of magnesian clusters in the ribbons is discounted. An homogeneous distribution of the octahedral cations (Al, Fe³⁺ and Mg) along the ribbons is proposed.

Key Words—Esquivias, FTIR Spectroscopy, Mg-palygorskite, Octahedral Occupancy, Palygorskite, Spain, Tajo Basin.

INTRODUCTION

Palygorskite is a fibrous clay mineral, the structure of which consists of ribbons of a 2:1 phyllosilicate structure, linked by periodical inversion of the apical oxygens of the continuous tetrahedral sheet and thus the octahedral sheet is discontinuous. Bradley (1940) proposed the first structural pattern for palygorskite and suggested that the mineral has the formula $\text{Si}_8\text{Mg}_5\text{O}_{20}(\text{OH})_2(\text{OH}_2)_4\cdot 4\text{H}_2\text{O}$. When Al is incorporated into the structure, it can fill any of the five octahedral positions leaving vacancies.

The structural model proposed by Bradley has been followed by others. Drits and Alexandrova (1966) published a revision of chemical analyses of palygorskites, concluding that in most cases, only four of each five octahedral positions can be occupied. Therefore they suggested a dioctahedral model, as opposed to the trioctahedral one postulated by Bradley. Later, Drits and Sokolova (1971) confirmed the dioctahedral model, so that in the octahedral sheet, a position (the middle one) would be empty. This model has also been proposed by Mifsud *et al.* (1978) based on chemical and thermal analysis of samples from different localities. According to Serna *et al.* (1977) the number of octahedral positions per unit-cell in palygorskite is five, although it does not seem possible that all can be filled. In most palygorskites, only four of each five positions are filled, whereas some seem to be completely dioctahedral palygorskites.

Thus, the structural formula is $\text{Si}_8(\text{Mg}_2\text{Al}_2)\text{O}_{20}(\text{OH})_2(\text{OH}_2)_4\cdot 4\text{H}_2\text{O}$.

Although palygorskite is relatively rare, it occurs in a great variety of environments. It is an authigenic mineral commonly formed in lacustrine environments or in soils, and it occasionally appears in marine environments or associated with hydrothermal activity. Its occurrence is also frequently reported from calcrites, caliches or carbonate-rich soils (Verrecchia and Le Coustumer, 1996). The general conditions of palygorskite stability have been discussed by Singer and Norrish (1974), Weaver and Beck (1977) and Jones and Galán (1991).

Numerous authors have mentioned the presence of palygorskite in Spanish Tertiary basins. Torres-Ruiz *et al.* (1994) made a revision of the geochemistry of sepiolite-palygorskite Spanish Neogene deposits. The three most important deposits are: Lebrija (southeastern Spain), studied by González and Galán (1984) and Galán and Ferrero (1982), and mined over hundreds of years for its use as a clarifying agent in wines; Torrejón (Cáceres), reported by Galán and Castillo (1984); and Bercimuel (Segovia) studied by Suárez *et al.* (1994 and 1995). The last is the only one still active. Few crystallochemical data have been reported for these occurrences.

The presence of palygorskite in Esquivias has been mentioned in several papers (Pozo *et al.*, 1985; Leguey *et al.*, 1985; García Romero, 1988, among others), but none presents chemical or structural data. The aim of this work is to crystallographically characterize the Esquivias palygorskite, which, in comparison to all other published data, has an anomalous chemical composition.

* E-mail address of corresponding author:
mromero@geo.ucm.es
DOI: 10.1346/CCMN.2004.0520409

These Mg-clay deposits are widely distributed within lacustrine and distal alluvial fan deposits from the Intermediate Unit (Miocene) of the Madrid Basin. To the northeast of Esquivias (Figure 1), thin (30 cm thick) argillaceous beds are interlayered with calcretes/palustrine limestones. The palygorskite studied occurs in all these rocks mixed with calcite and other minerals, mainly sepiolite and opal (Bellanca *et al.*, 1992; Bustillo and García Romero, 2003). In the thin argillaceous beds, palygorskite coexists with sepiolite and smectites, but at the top it occurs alone and it is possible to obtain good samples. Palygorskite formed by direct precipitation from interstitial waters present in the calcretes/palustrine limestones. Part of the palygorskite included in these rocks formed later than calcite, and its formation may have been favored by the dissolution of calcite. There were very large amounts of Mg and Si available in the Madrid Basin, as indicated by the important deposits of Mg-bentonite and sepiolite, and the presence of important silicifications.

MATERIALS AND METHODS

Apart from the samples from Esquivias, we also analyzed palygorskites from Attapulgus (Georgia, USA), Bercimuel (Segovia, Spain) and Torrejón el Rubio (Cáceres, Spain), in order to make a comparative study, and to use them as references. These palygorskites have been studied widely and reported in the literature.

Mineralogical characterization was performed by X-ray diffraction (XRD) using a Siemens D-500 XRD diffractometer with CuK α radiation and a graphite monochromator. The samples used were random powder specimens scanned from 2 to 65°20 at 0.02°20/3 s scan speed.

Particle morphology and textural relationships were established using scanning electron microscopy (SEM) and transmission electron microscopy (TEM). The SEM observations were performed using a JEOL JSM 6400 microscope, operating at 20 kV and equipped with a Link System energy dispersive X-ray (EDX) micro-analyser. Prior to SEM examination, freshly fractured surfaces of representative samples were air dried and coated with Au under vacuum in an Ar atmosphere. The TEM observations were performed by depositing a drop of diluted suspension on a microscopic grid with collodion and coated with Au.

The chemical composition was obtained using analytical electron microscopy (AEM) with TEM, in samples of great purity, using a JEOL 2000 FX microscope equipped with a double-tilt sample holder (up to a maximum of ±45°) at an acceleration voltage of 200 kV, with 0.5 mm zeta-axis displacement and 0.31 nm point-to-point resolution. The microscope incorporates an OXFORD ISIS EDX spectrometer (136 eV resolution at 5.39 keV) and has its own software for quantitative analysis.

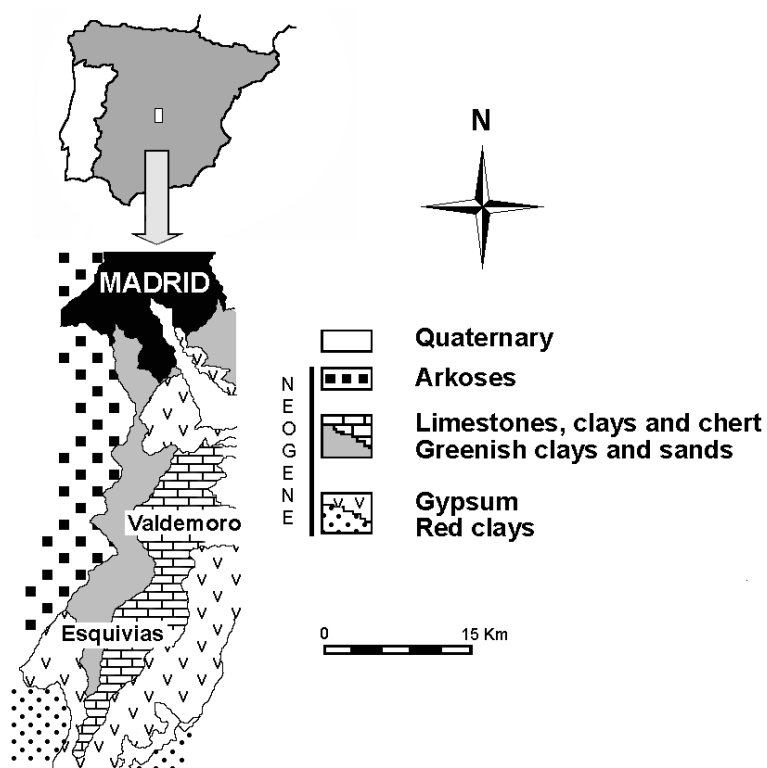


Figure 1. Geographic location and outcrop map of the Esquivias area.

The structural formulae for palygorskite were calculated on the basis of 21 oxygens per unit-cell. All the Fe present was considered as Fe^{3+} (owing to the limitation of the technique), but the possible existence of Fe^{2+} should be taken into account.

The FTIR spectra were recorded in the 4000 to 500 cm^{-1} ranges on a BRUKER EQUINOX 55 spectrometer. The samples were prepared using the KBr pellet technique.

RESULTS

The samples studied contain palygorskite, calcite and quartz. Some samples are composed almost exclusively of palygorskite, whereas others have considerable amounts of calcite (up to 30%). Quartz is <5% in all samples and no other phyllosilicates were identified. Figure 2 shows a representative diffraction pattern of Esquivias palygorskite.

Scanning electron micrographs of fracture surfaces reveal the characteristic fibrous morphology of the palygorskite (Figure 3a). The aggregates grow as dense fiber masses connected to each other in pure palygorskite beds, or enmesh the calcite crystals and sprout out from their surfaces, cover them, and fill totally or partially the voids between carbonates. The fibers have an average length of 1–2 μm , and their diameters may vary between 0.15 and 0.5 μm (Figure 3b).

The TEM images of dispersed Esquivias palygorskite show mainly: (1) aggregates of fibers grouped parallel to their c axis, giving rise to particles of greater size; and (2) fibers growing over crystals of calcite. Detailed observations of individual fibers allow us to see that

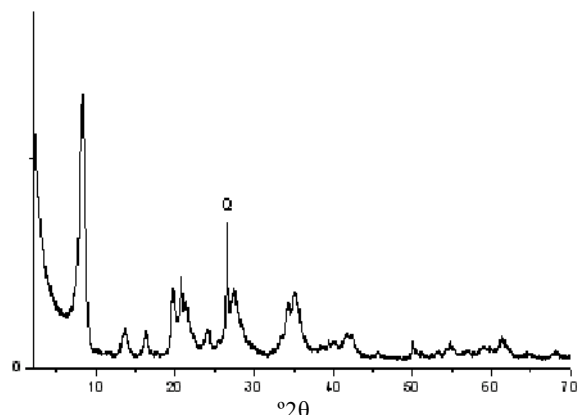


Figure 2. Random powder XRD patterns of the Esquivias palygorskite. Q = quartz. All peaks other than that for quartz belong to palygorskite.

smaller units form each one of them. In the same way, the smaller units are arranged parallel. Amorphous phases have not been detected.

Table 1 shows structural formulae calculated from AEM of isolated clay particles of Esquivias samples and Table 2 those corresponding to Attapulgus, Bercimuel and Torrejón. The mean structural formula obtained for Esquivias palygorskite was $(\text{Si}_{7.87}\text{Al}_{0.13})\text{O}_{20}(\text{Al}_{1.04}\text{Fe}_{0.20}^{3+}\text{Mg}_{3.11}\square_{0.65})(\text{OH})_2(\text{OH}_2)_4(\text{Ca}_{0.02}\text{K}_{0.05}\text{Na}_{0.08})$. Esquivias samples are the richest in octahedral Mg. The values of Mg atoms per half unit-cell range from 2.73 to 3.86, with a mean value of 3.11, whereas, as is shown, the total number of atoms of Mg from the reference samples studied does not exceed 2.47 atoms per half unit-cell (Attapulgus (2.06–2.47), Bercimuel

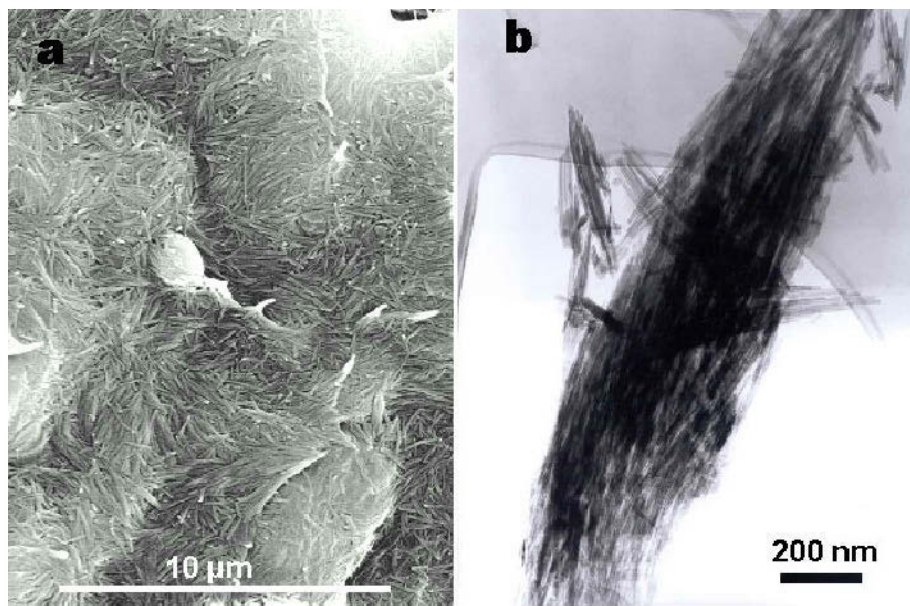


Figure 3. Esquivias palygorskite: (a) SEM image of fibers growing tightly. (b) TEM image of fibers arranged to form aggregates.

Table 1. Structural formulae from the Esquivias palygorskite samples, calculated from EDS analyses of isolated palygorskite particles. The number of cations is on the basis of $O_{20}(OH)_2(OH_2)_2$.

	Si	^{IV} Al	Σt	^{VI} Al	Fe ³⁺	Mg	Ti	Σo	Ca	K	Na
1	7.97	0.03	8.00	1.03	0.14	3.26		4.43		0.01	0.02
2	7.93	0.07	8.00	1.07	0.19	3.15		4.41			
3	7.71	0.29	8.00	1.29	0.26	2.73		4.28	0.04	0.10	
4	7.98	0.02	8.00	1.07	0.22	3.08		4.37			
5	7.98	0.02	8.00	1.07	0.15	3.18		4.40			
6	7.92	0.08	8.00	1.04	0.17	3.23		4.44			
8	7.93	0.07	8.00	0.96	0.17	3.30		4.43	0.02	0.03	
9	7.89	0.11	8.00	0.73	0.06	3.86		4.65			
10	7.97	0.03	8.00	0.94	0.20	3.16		4.30	0.13	0.04	
21	7.85	0.15	8.00	1.05	0.10	3.32		4.47	0.01	0.04	
22	7.77	0.23	8.00	0.98	0.21	3.07	0.03	4.29	0.02	0.06	0.32
23	7.78	0.22	8.00	1.09	0.21	2.98	0.02	4.30	0.02	0.06	0.21
24	7.75	0.25	8.00	1.04	0.24	3.04	0.02	4.34	0.04	0.12	0.08
25	7.79	0.21	8.00	1.11	0.32	2.73	0.02	4.18	0.04	0.12	0.19
26	7.90	0.10	8.00	1.06	0.19	3.07		4.32	0.02	0.05	0.13
27	7.90	0.10	8.00	1.15	0.21	2.90		4.26	0.05	0.08	0.02
28	7.80	0.20	8.00	1.06	0.28	2.92	0.04	4.30	0.02	0.06	0.09
29	7.92	0.08	8.00	0.92	0.20	3.28		4.40	0.01	0.07	0.08
30	7.69	0.31	8.00	0.98	0.20	3.27		4.45	0.01	0.05	0.20
31	7.88	0.12	8.00	1.20	0.26	2.73		4.19	0.02	0.08	0.16
Mean	7.87	0.13	8.00	1.04	0.20	3.11	0.01	4.36	0.02	0.05	0.08

(1.74–2.39) and Torrejón (2.12–2.32)). The degree of octahedral occupancy is also very different, the sum of

octahedral cations of the Esquivias palygorskite ranges from 4.19 to 4.65 and the mean value per half unit-cell is

Table 2. Structural formulae from reference palygorskite (Attapulgus, Bercimuel and Torrejón) samples, calculated from EDS analyses of isolated palygorskite particles. The number of cations is on the basis of $O_{20}(OH)_2(OH_2)_2$.

	Si	^{IV} Al	Σt	^{VI} Al	Fe ³⁺	Mg	Ti	Σo	Ca	K	Na
Att.1	7.74	0.26	8.00	1.55	0.32	2.07		3.94	0.16	0.09	0.06
Att.2	7.98	0.02	8.00	1.37	0.23	2.45	0.02	4.05	0.07	0.12	0.03
Att.3	7.84	0.16	8.00	1.50		2.22		3.72	0.09	0.05	0.19
Att.4	7.92	0.08	8.00	1.40	0.23	2.45	0.01	4.08	0.06	0.02	0.15
Att.5	7.83	0.17	8.00	1.52	0.25	2.34		4.11	0.08	0.04	
Att.6	7.82	0.18	8.00	1.42	0.31	2.29		4.02	0.09	0.04	0.21
Att.7	7.85	0.15	8.00	1.44	0.25	2.47		4.16	0.04	0.04	
Att.8	7.81	0.16	7.97	1.48	0.28	2.35		4.11	0.07	0.03	
Att.10	7.90	0.10	8.00	1.59	0.35	2.06		4.00	0.06	0.04	
Mean	7.85	0.14	8.00	1.47	0.25	2.30	0.00	4.02	0.08	0.05	0.07
Ber.1	7.88	0.12	8.00	1.78	0.36	1.74		3.88	0.09	0.05	
Ber.2	7.79	0.21	8.00	1.66	0.38	1.96		4.00	0.08	0.02	
Ber.4	7.84	0.16	8.00	1.82	0.37	1.69		3.88	0.05	0.09	
Ber.5	7.80	0.20	8.00	1.63	0.35	2.04		4.02	0.06	0.06	
Ber.7	7.97	0.03	8.00	1.36	0.39	2.39		4.14			
Ber.6	8.09		8.09	1.37	0.46	2.04		3.87	0.03		
Mean	7.90	0.12	8.02	1.60	0.39	1.98		3.97	0.05	0.04	
Tor.1	8.02		8.02	1.50	0.30	2.26		4.06			
Tor.2	7.81	0.19	8.00	1.53	0.39	2.12		4.04	0.01	0.10	
Tor.3	7.85	0.15	8.00	1.47	0.37	2.29		4.13	0.03	0.04	
Tor.5	7.93	0.07	8.00	1.52	0.41	2.15		4.08			
Tor.5	7.97	0.03	8.00	1.44	0.37	2.31		4.12			
Tor.6	8.01		8.01	1.40	0.39	2.29		4.08			
Tor.8	7.82	0.18	8.00	1.52	0.32	2.31		4.15	0.01	0.07	
Tor.10	7.88	0.12	8.00	1.39	0.44	2.32		4.15			
Tor.11	7.91	0.09	8.00	1.51	0.37	2.23		4.11			
Mean	7.91	0.09	8.00	1.48	0.37	2.25		4.10	0.01	0.02	

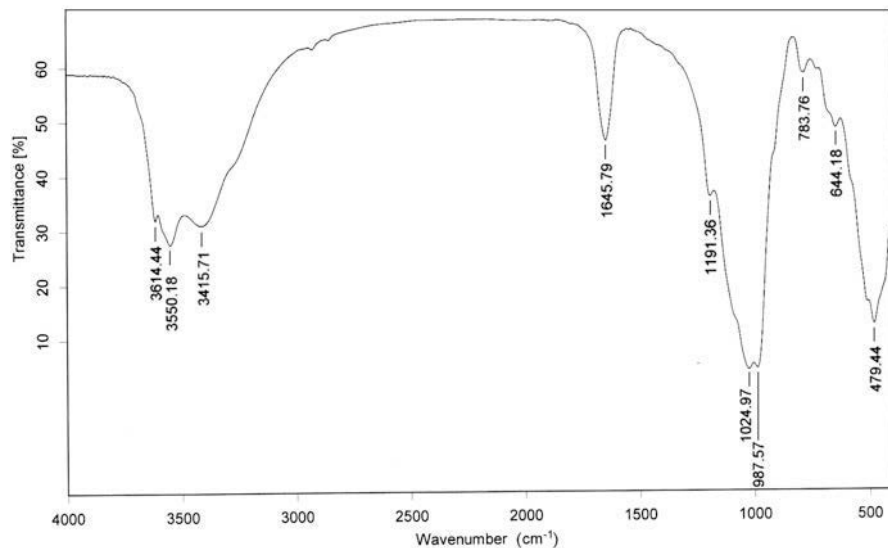


Figure 4. FTIR spectrum of the Esquivias palygorskite.

4.36 atoms. However, the sum of octahedral cations per half unit-cell ranges from 3.72 to 4.16 for the Attapulgus palygorskite, from 3.87 to 4.14 for Bercimuel palygorskite, and from 4.04 to 4.15 for Torrejón palygorskite; the mean values of number of octahedral cations are 4.02, 3.97 and 4.10, respectively.

The FTIR spectrum of the Esquivias palygorskite is shown in Figure 4. The spectra for the Esquivias and reference samples are similar, but some important differences are found both in the intensity and in the position of the peak, especially in the region of minor wavenumbers. The positions of the bands corresponding to the four studied samples are listed in Table 3. In addition to the palygorskite bands, the three reference samples present bands corresponding to quartz (776–798 cm⁻¹), and the Torrejón palygorskite presents those characteristic of calcite at 1433 and 876 cm⁻¹ (Farmer, 1974).

DISCUSSION

The XRD patterns of pure palygorskite from Esquivias show the characteristic reflections of this mineral. The peaks are broader than those of the other palygorskites studied, probably due both to the small size of the particles and their poor crystallinity. With electron microscopy, the Esquivias palygorskite shows its characteristic fibrous morphology.

The Esquivias palygorskite is very rich in Mg according to the structural formula obtained by AEM. A comparative study of literature analyses (Table 4 shows 47 structural formulae for palygorskite), reference analyses (Table 2) and Esquivias analyses (Table 1) indicates that the Esquivias palygorskite has the largest number of Mg atoms of all the samples considered. The Esquivias palygorskite is also the sample with largest

number of octahedral positions occupied, in part related to the high Mg content, which means that a higher occupancy is needed to complete the layer charge.

The octahedral cations of Esquivias palygorskite (Table 1) are mainly divalent (Mg from 2.73 to 3.86 atoms per half unit-cell) and minor trivalent cations (Al from 0.73 to 1.29 and Fe³⁺ from 0.10 to 0.32 atoms per half unit-cell). Table 5 illustrates a comparative study of palygorskite octahedral cations, and it shows the high Mg concentration of the Esquivias palygorskites.

Table 3. Positions (wavenumbers, cm⁻¹) of bands and shoulders (*) found in FTIR spectra of the Esquivias and reference samples.

Esquivias	Attapulgus	Bercimuel	Torrejón
3614	3615	3615	3614
3592*		3588*	3577*
3550	3547	3545	3548
			3473*
3416	3422	3423	3415
3296*	3250*	3255*	3227
1639	1652	1643	1639
1617			1619
			1433
1191	1194	1199*	
	1141*	< infl	1198*
1091	1091	< infl	1127*
1025	1032	1028	1095*
987	987	993	1033
	913	918	987
			876
784	Q(776-798)	Q(776-798)	Q(776-798)
729			
683*	673	699	693
644	648	647	645
584*	658	< infl	583
515*	514	512	511
479	481	480	478

Table 4. Structural formulae for palygorskite taken from examples in the literature: 1–11 compiled by Newman and Brown, (1978); 12–14 from Galán and Carretero (1999); 15–37 compiled by Galán and Carretero (1999); 38–43 from Torres-Ruiz *et al.* (1994); 44 from López Galindo *et al.* (1966); 45 from Verrecchia and Le Coustumer (1996); 46 from Imai and Otsuka (1984); 47 from Hasnuddin Siddiqui (1984); and 48 from Chahi *et al.* (2002).

	Si	^{IV} Al	Σt	^{VI} Al	Fe ³⁺	Mg	Ti	Fe ²⁺	Σo	Ca	K	Na
1	7.34	0.66	8.00	2.25	0.17	1.47			3.89	0.21		
2	7.75	0.25	8.00	2.35	0.17	1.29			3.81	0.06		
3	7.61	0.39	8.00	2.26	0.23	1.43			3.92	0.02		
4	7.71	0.29	8.00	2.00	0.01	1.70			3.71		0.08	0.08
5	7.50	0.50	8.00	1.62	0.41	1.78			3.81	0.34		
6	8.06		8.06	2.00	0.05	1.62			3.67	0.08	0.01	0.04
7	7.80	0.20	8.00	1.51	0.38	2.22			4.11		0.09	
8	7.82	0.18	8.00	1.57	0.20	2.04			3.81	0.36		
9	8.09		8.09	1.57	0.00	2.24			3.81	0.12	0.14	0.07
10	7.88	0.12	8.00	0.95	0.42	2.81	0.10		4.28			
11	7.75	0.25	8.00	0.12	0.10	3.84	0.08		4.14	0.17	0.04	0.21
12	7.71	0.29	8.00	1.43	0.56	2.10			4.09			
13	7.86	0.14	8.00	1.84	0.40	1.71			3.95			
14	8.05		8.05	1.46	0.41	2.09			3.96			
15	7.81	0.19	8.00	1.40	0.48	1.99			3.87	0.04	0.06	0.32
16	7.80	0.20	8.00	1.13	0.87	1.83			3.83	0.14	0.23	0.03
17	7.66	0.34	8.00	1.52	0.15	2.65			4.32	0.04	0.04	
18	8.05		8.05	1.68	0.10	2.20			3.98	0.02		
19	7.85	0.15	8.00	1.15	0.38	2.53	0.08		4.14			
20	7.98	0.21	8.19	1.29	0.37	1.96		0.03	3.62	0.32		
21	7.89	0.11	8.00	1.87	0.16	1.91			3.94	0.05		0.03
22	7.64	0.36	8.00	1.73	0.63	1.45			3.81	0.08		
23	7.79	0.21	8.00	1.52	0.31	1.89	0.05		3.77	0.31	0.05	0.08
24	7.43	0.57	8.00	1.58	0.65	1.66			3.89	0.06	0.21	0.14
25	7.35	0.65	8.00	1.29	0.47	2.20			3.96	0.20	0.12	0.45
26	7.66	0.34	8.00	1.48	0.46	2.02	0.03		3.99	0.05	0.15	0.13
27	7.58	0.42	8.00	0.87	0.81	2.42	0.08		4.18	0.08	0.08	0.03
28	7.50	0.50	8.00	1.68	0.54	1.77			3.99		0.27	
29	7.79	0.21	8.00	1.06	0.56	2.46	0.02		4.10	0.06	0.06	0.03
30	7.70	0.30	8.00	1.27	0.63	2.06	0.06		4.02	0.06	0.06	0.05
31	7.86	0.14	8.00	2.11	0.22	1.12			3.45	0.43		
32	7.64	0.36	8.00	2.27	0.23	1.40			3.90	0.02		
33	7.61	0.39	8.00	1.81		2.52			4.33	0.04		
34	7.33	0.67	8.00	2.37		1.69			4.06	0.08		
35	7.99	0.01	8.00	1.62	0.05	1.90	0.05	0.45	3.62		0.08	
36	8.04		8.04	1.05	0.08	2.75			3.88	0.08		
37	7.52	0.48	8.00	2.08	0.17	1.37	0.04		3.66	0.15	0.30	0.16
38	8.00		8.00	1.22	0.66	1.75	0.09		3.72		0.05	0.05
39	8.00		8.00	1.13	0.63	1.98	0.08		3.82	0.03	0.06	0.05
40	7.20	0.80	8.00	1.36	1.31	1.07	0.11		3.85		0.07	0.15
41	7.37	0.63	8.00	1.12	1.16	1.43	0.09		3.80	0.19	0.06	0.13
42	8.00		8.00	1.29	0.38	2.24	0.06		3.97	0.00	0.05	0.02
43	8.00		8.00	1.16	0.37	2.43	0.06		4.02	0.08	0.05	0.03
44	7.79	0.21	8.00	1.64	0.42	1.90			3.96	0.03	0.12	
45	8.01		8.01	1.61	0.53	2.35			4.49	0.11	0.28	
46	7.83	0.17	8.00	1.58	0.19	2.04		0.03	3.84	0.36		
47	7.80	0.20	8.00	1.13	0.87	1.83			3.83	0.14	0.23	0.03
48	8.00		8.00	1.19	0.33	2.60			4.12	0.06	0.10	0.02
Mean	7.76	0.25	8.01	1.52	0.39	1.99	0.02	0.01	3.94	0.10	0.07	0.05

Although Bradley (1940) proposed the possibility of trioctahedral palygorskite, at present the accepted model has palygorskite intermediate between di and trioctahedral phyllosilicate (Bailey, 1980; Drits and Aleksandrova, 1966; Paquet *et al.*, 1987), with 21 oxygens for a half, dehydrated, unit-cell, with formula: $(\text{Si}_{8-x}R_x^{3+})(\text{Mg}_{5-y-z}R_y^{3+}\square_z)\text{O}_{20}(\text{OH}_2)(\text{OH}_2)_4R_{(x-y-z)/2}^{2+} \cdot 4\text{H}_2\text{O}$. On average, four of each

five octahedral positions are occupied. According to Newman and Brown (1987), the sum of octahedral cations lies between 3.76 and 4.64, with a mean value of 4.00, indicating that palygorskite should be classed as a dioctahedral mineral. Al, Fe³⁺ and Fe²⁺ are the main elements which substitute for Mg. The Esquivias palygorskite has the largest sum of octahedral cations (4.36)

Table 5. Octahedral occupancy ranges (maximum, minimum and means values), from the literature, patterns and Esquivias samples. $V^I(R^2+R^3)$ = octahedral cations other than Mg; they are mainly Al and Fe^{3+} .

	Octahedral cations	$V^I Mg$	$V^I(R^2+R^3)$	Mg/Al	Si/Mg	$Mg/(Al+Fe^{3+})$
Literature	3.62–4.49 (3.94)	0.93–3.08 (1.99)	1.12–2.67 (1.91)	1.37	4.04	1.06
Attapulgus	3.72–4.16 (4.02)	2.06–2.47(2.30)	1.50–1.94 (1.72)	1.44	3.43	1.35
Torrejón	4.04–1.15 (4.10)	2.12–2.32(2.25)	1.79–1.93 (1.85)	1.19	4.04	1.01
Bercimuel	3.87–4.14 (3.97)	1.69–2.39(1.98)	1.75–2.19 (1.99)	1.44	3.51	1.22
Esquivias	4.18–4.65 (4.36)	2.73–3.86(3.11)	0.79–1.55 (1.24)	2.72	2.54	2.58

compared with reference samples and literature analyses (with the exception of sample 45 (Table 4) from Verrecchia and Le Coustumer (1996)), the Mg constitutes between 29 and 79% of the octahedral cations and Al between 28 and 59%. Newman and Brown (1987) affirm that octahedral cations range from ~2½ trivalent plus 1½ divalent from samples abundant in Al, to 1½ trivalent with 2½ divalent for the palygorskite from Queensland (sample 10, Table 4), and even to ½ trivalent with 4½ divalent for a highly magnesian sample (sample 11, Table 4, from the Volhynia basalts, USSR, Drits and Aleksandrova, 1966). By comparison with these authors and with the literature analyses, the Esquivias palygorskite has the highest proportion of Mg, comparable only to the highly magnesian sample from Drits and Aleksandrova (1966). Likewise, Esquivias palygorskite shows a Mg/Al and Mg/Si ratio double that of reference and bibliography samples.

The ratio between divalent and trivalent octahedral cations $R2/R3$ ($Mg/Al+Fe^{3+}$) in palygorskite analyses from Attapulgus, Bercimuel and Torrejón has average values close to 1 (1.35, 1.01 and 1.22 respectively). Galán and Carretero (1999) affirmed that palygorskite contains mainly Mg, Al and Fe with an $R2/R3$ ratio close to 1, similar to the value found in our reference samples. The Esquivias samples show an $R2/R3$ of 2.58 (Table 5).

Moreover, this mineral can contain variable amounts of other cations, such as Na, Ca and K as exchange cations. Some authors, such as Velde (1985) and Galán

and Carretero (1999), suggest that the presence of cations such as Ca, K and Na in the analyses of palygorskite is probably due to impurities (calcite, illite) and they are not exchange cations. However, palygorskite is composed of very small fibers and for this reason, the particle edges have a strong influence on its ionic exchange capacity. Besides, the coordination of octahedral cations at each edge of the octahedral sheet is completed with two water molecules and therefore allows new cations to be bonded to these water molecules in the particle edges. Thus, palygorskite has exchange capacities in the region of 57–300 $\mu eq\ g^{-1}$ (Newman and Brown, 1987).

The chemical data are plotted on different diagrams as shown in Figure 5 (Si/Mg vs. $R3/R2$) and Figure 6 ($(Al+Fe^{3+})^V$ vs. Mg). In both cases, the reference and bibliography samples are distributed through a similar domain, but in contrast, the Esquivias samples plot in a separate domain. On Figure 5 we also plotted sepiolite chemical data from Newman and Brown (1978). It is noticeable here that the Esquivias data plot between the palygorskite and sepiolite samples.

The aim of the FTIR spectroscopic study is to gain knowledge of the environment of the octahedral cations. The FTIR spectra of Esquivias palygorskites and the other samples studied are similar both in the position of the bands and in intensity. There are three bands at 3615, 3548 and $3420\ cm^{-1}$ and two shoulders at 3580 and

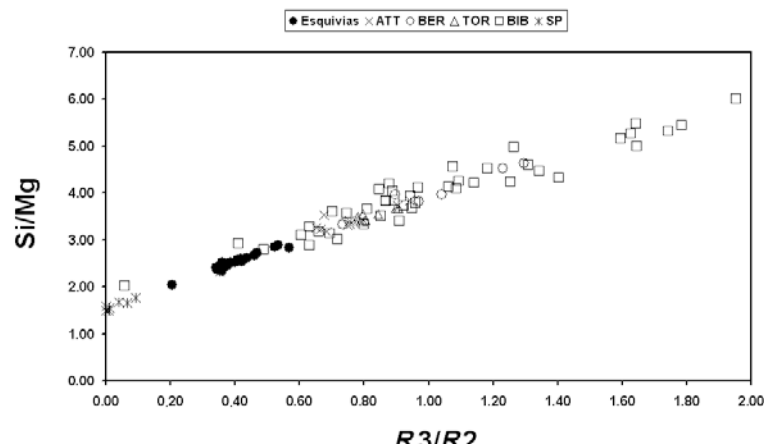


Figure 5. Relationship between Si/Mg and $R3/R2$ ($Al+Fe^{3+}/Mg$) cations of palygorskite samples (Esquivias, reference and bibliography) and sepiolite chemical data from Newman and Brown (1978). ATT = Attapulgus, BER = Bercimuel, TOR = Torrejón el Rubio, BIB = bibliographic data, SP = sepiolite.

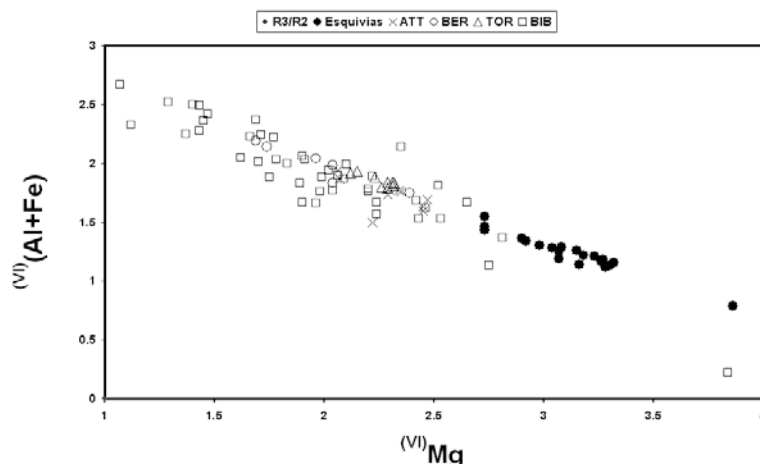


Figure 6. Relationship between $(\text{VI})(\text{Al}+\text{Fe})$ and Mg of the Esquivias palygorskite and reference samples. Abbreviations as in Figure 5.

3250 cm^{-1} . The bands are due to the presence of different types of water molecules in the structure of the clay (coordinated and zeolitic water), and to the presence of OH groups coordinated to metallic cations. These bands and shoulders are reported in the literature for these and other palygorskites. The coincidence in the position of the band at 3615 cm^{-1} which always appears in palygorskite (both in the studied samples and in those from the literature) but not in sepiolite studies is especially significant. This band is assigned to the stretching mode of the structural hydroxyls bonded to the different cations (M_3 -OH stretching) mainly Al, in an octahedral coordination (Mendelovich, 1973; Serna *et al.*, 1977; Khorami and Lemieux, 1989; Vicente González *et al.*, 1996; Ausburger *et al.*, 1998; and Frost *et al.*, 2001).

For a theoretical palygorskite with structural formula $\text{Si}_8(\text{Mg}_2\text{Al}_2)\text{O}_{20}(\text{OH})_2(\text{OH}_2)_4\cdot 4\text{H}_2\text{O}$, Güven (1992) proposed the configuration of the octahedral ribbons plotted in Figure 7a, with M_1 , M_2 and M_3 sites, where M_3 is occupied by Mg, M_2 is occupied by Al or Fe and M_1 sites are vacant, and the band at 3615 cm^{-1} is due to $\text{Al}_2\square\text{-OH}$ or $\text{AlFe}\square\text{-OH}$. Also, values of $3620\text{--}3614 \text{ cm}^{-1}$ are reported for other dioctahedral configurations such as $\text{AlMg}\square\text{-OH}$, and $\text{Mg}_2\square\text{-OH}$, the latter in sepiolite (Hayasi *et al.*, 1969; Prost, 1973; Frost *et al.*, 2001). The Esquivias palygorskite does not show a band at 3680 cm^{-1} ; this is known to be due to OH-stretching in $\text{Mg}_3\text{-OH}$ in a trioctahedral structure (Frost *et al.*, 2001 and previous works) although this sample has a very high Mg content and the octahedral occupancy is close to trioctahedral.

The distribution of Mg, Al and Fe ions and of the vacancies in the ribbon of the palygorskite is plotted in Figure 7 using the scheme of Güven (1992) and taking into account the mean values obtained for the structural formulae of the Esquivias palygorskite. Two possibilities are taken into account: (1) the vacancies, the Al and the small Fe content are distributed homogeneously in the

M_2 positions (Figure 7b); (2) the distribution is made assuming the existence of trioctahedral clusters, *i.e.* the existence of Mg in M_2 positions (Figure 7c). With this latter possibility, $\sim 33\%$ of the ribbon is trioctahedral, and as a consequence of this, a small band at 3680 cm^{-1} should be observed in the IR spectra, but this band is not found. In the model proposed in Figure 7b the high Mg content can be distributed without trioctahedral domains. The Mg occupies M_3 , M_2 and also M_1 positions but there is no $\text{Mg}_3\text{-OH}$ configuration. However, this model presents a small part of the ribbon with an excess of octahedral charge which can be compensated by the location of the tetrahedral substitution (Si for Al) in the same region. Thus, the distribution of the large number of octahedral cations in the structure of the Esquivias palygorskite is only possible with a highly ordered arrangement in the octahedral sheet.

In the minor wavenumbers' region of the IR spectra there are important differences between the Esquivias palygorskite and other samples. The bands corresponding to impurities are also found. Two bands centered at 798 and 776 cm^{-1} , characteristic of quartz, are present in the three reference samples and, in the Torrejón palygorskite, two bands at 1453 and 880 cm^{-1} corresponding to calcite are also found. Between 1200 and 400 cm^{-1} , bands characteristic of silicate can be observed, mainly those corresponding to Si-O bonds in the tetrahedral sheet, and also to M-O-stretching vibrational bonds. This region of the spectra is very complex because the lattice modes also contribute, but it is especially interesting because it provides information about the nature of the octahedral sheet. In a recent study that takes into account the lattice dynamic calculations for the palygorskite structure (McKeown *et al.*, 2002), it is considered that "above $\sim 700 \text{ cm}^{-1}$ in the IR spectra, the eigenmodes are dominated by atomic displacements within the silicate sheets. Below 700 cm^{-1} the eigenmodes become mixed with motions among the Mg octahedra and the silicate sheets. As mode frequencies

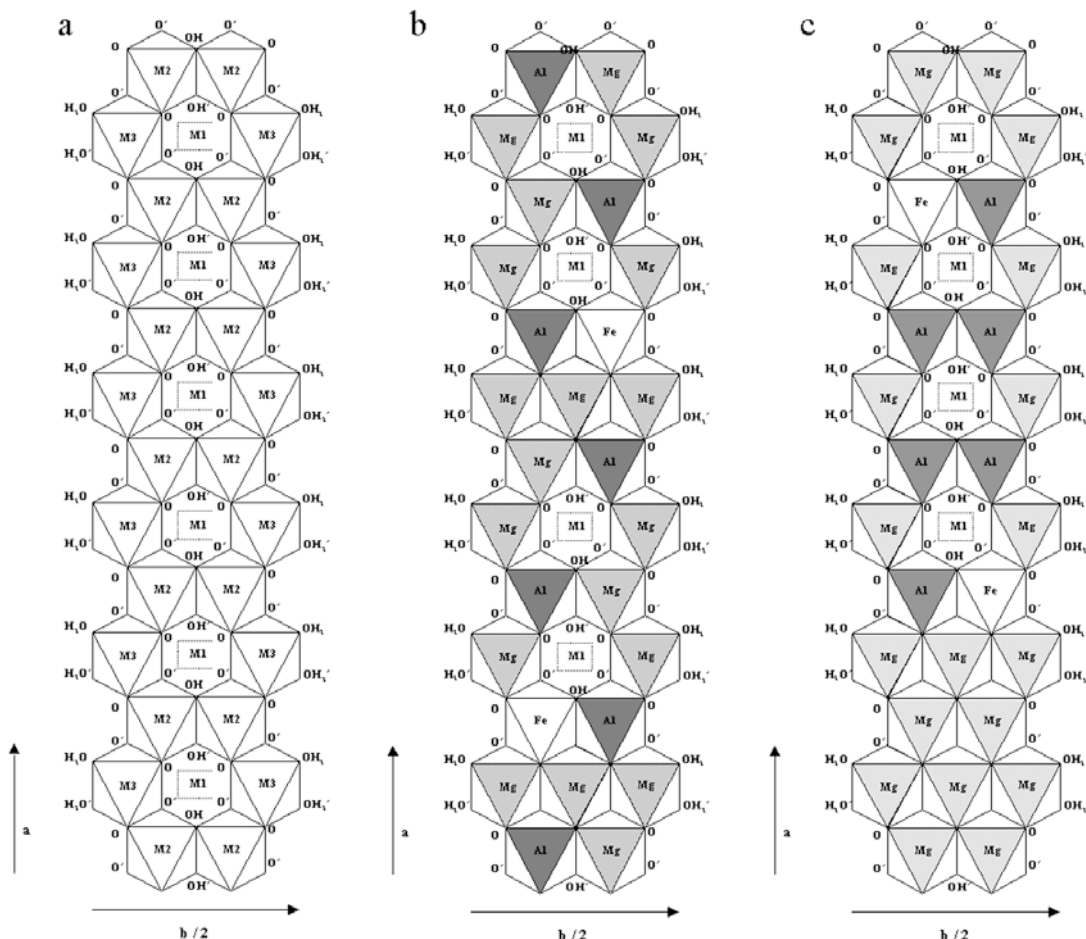


Figure 7. (a) Configuration of the octahedral ribbons in the palygorskite structure having M_1 , M_2 and M_3 octahedral sites after Güven (1992). O' , O'' , OH' and H_2O' belong to the top triangles of the octahedra in this projection. (b) Possible distribution of the octahedral cations in the Esquivias palygorskite with the Mg distributed homogeneously along the fiber. (c) Possible distribution of the octahedral cations in the Esquivias palygorskite with the Mg distributed in clusters.

decrease, the corresponding eigenmodes evolve from more localized Mg–O stretch, O–Mg–O bend and O–Si–O bend motions to longer-range motions such as silicate sheet deformations caused by silicate tetrahedra rotation and silicate sheet shearing around the Mg-octahedral sheets". In this region, in the sequence of Si–O–M–O–Si bonds, a very important factor is the nature of M (Mg, Al, Fe...) while the trioctahedral or dioctahedral surrounding has less influence. In the reference samples the Mg, Al and Fe contents are similar and their influence produces different bands due to the possible M – M –OH and M – M –O bonds. Chahí *et al.* (2002) attribute the bands at 911, 867 and 834 cm⁻¹ to Al–Al–OH, Al–Fe–OH and Al–Mg–OH, respectively. In the Esquivias palygorskite, a simpler aspect is observed in this region of the spectra due to preponderance of Mg in the octahedral sheet, the more intense bands are due to high Mg content: Mg–Mg–O at 648 cm⁻¹ and Mg–Mg–OH or Mg–(Al,Fe)–OH at 784 cm⁻¹ (Augsburger *et al.*, 2001).

Only one other possibility can be suggested: a possible random intergrowth between palygorskite and sepiolite such as that reported by Martín Vivaldi and Linares González (1962) in the bentonites of Cabo de Gata (Almería, Spain), but this sepiolite should have a large number of octahedral vacancies.

CONCLUSIONS

The Esquivias palygorskite has the highest Mg content reported in the literature to date. Chemically, this palygorskite could fill the compositional gap existing between sepiolite and palygorskite. The FTIR studies show that this is possible without the existence of Mg₃–OH bonds. No Mg pure clusters are found, though octahedral occupancy is very high (90%), with a percentage similar to the other trioctahedral clay minerals. The distribution of the large number of octahedral cations in the structure of the Esquivias palygorskite is only possible with a highly ordered

arrangement in the octahedral sheet and an homogeneous distribution of different octahedral cations and vacancies along the octahedral sheet is proposed.

ACKNOWLEDGMENTS

The authors thank Dr Angela Arteaga for technical assistance and are also very grateful to Dr Arieh Singer and Dr Blair Jones for their constructive comments. Financial support by CICYT (project BTE2002-04017-CO2) is acknowledged.

REFERENCES

- Augsburger, M.S., Strasser, E., Perino, E., Mercader, R.C. and Pedregosa, J.C. (1998) FTIR and Mössbauer investigation of a substituted palygorskite: silicate with a channel structure. *Journal of Physical Chemical Solids*, **59**, 175–180.
- Bellanca, A., Calvo, J.P., Censi, P., Neri, R. and Pozo, M. (1992) Recognition of lake-level changes in Miocene lacustrine units, Madrid basin, Spain. Evidence from facies analysis, isotope geochemistry and clay mineralogy. *Sedimentary Geology*, **76**, 135–153.
- Bailey, S.W. (1980) Structure of layer silicates. Pp.1–123 in: *Crystal Structures of Clay Minerals and their X-ray Identification* (G.W. Brindley and G. Brown, editors). Monograph **5**, Mineralogical Society, London.
- Bradley, W.F. (1940) The structural scheme of attapulgite. *American Mineralogist*, **25**, 405–411.
- Bustillo, M.A. and García Romero, E. (2003) Arcillas fibrosas anómalas en encostramientos y sedimentos superficiales: características y génesis (Esquivias, Cuenca de Madrid). *Boletín Sociedad Española de Cerámica y Vidrio*, **42**, 289–297.
- Chahidi, A., Petit, S. and Decarreau, A. (2002) Infrared evidence of dioctahedral-trioctahedral site occupancy in palygorskite. *Clays and Clay Minerals*, **50**, 306–313.
- Drits, V.A. and Alexandrova, V.A. (1966) On the crystallographic nature of palygorskites. *Zapiski Vsesoyuznogo Mineralogicheskogo Obshchestva*, **95**, 551–560.
- Drits, V.A. and Sokolova, G.V. (1971) Structure of palygorskite. *Soviet Physics Crystallography*, **16**, 288–231.
- Farmer, V.C. (1974) *The Infrared Spectra of Minerals*. Monograph **4**, Mineralogical Society, London.
- Frost, R.L., Locos, O.B., Ruan, J. and Klopdroge, J.T. (2001) Near-infrared and mid-infrared spectroscopic study of sepiolites and palygorskites. *Vibrational Spectroscopy*, **27**, 1–3.
- Galán, E. and Carretero, I. (1999) A new approach to compositional limits for sepiolite and palygorskite. *Clays and Clay Minerals*, **47**, 399–409.
- Galán, E. and Castillo, A. (1984) Sepiolite-palygorskite in Spanish tertiary basins: Genetic patterns in continental environments. Pp. 87–124 in: *Palygorskite-Sepiolite. Occurrences, Genesis and Uses*. (A. Singer and E. Galán, editors). Developments in Sedimentology, **37**. Elsevier, Amsterdam.
- Galán, E. and Ferrero, A. (1982) Palygorskite-sepiolite clays of Lebrija, Southern Spain. *Clays and Clay Minerals*, **30**, 191–199.
- García Romero, E. (1988) Estudio mineralógico y estratigráfico de las arcillas de las facies centrales del Neógeno del borde sur de la Cuenca del Tajo. PhD thesis, Universidad Complutense, Madrid, Spain, 436 pp.
- González, M. and Galán, E. (1984) Mineralogía de los materiales terciarios del área de Tarazona-Borja-Ablitas (Depresión del Ebro). *Estudios Geológicos*, **40**, 115–128.
- Güven, N. (1992) The coordination of aluminum ions in the palygorskite structure. *Clays and Clay Minerals*, **40**, 457–461.
- Hasnuddin Siddiqui, M.K. (1984) Occurrence of palygorskite in the Deccan Trap Formation in India. Pp. 243–250 in: *Palygorskite-Sepiolite. Occurrences, Genesis and Uses* (A. Singer and E. Galán, editors). Developments in Sedimentology, **37**. Elsevier, Amsterdam.
- Hayasi, H., Otsuka, R. and Imai, N. (1969) Infrared study of sepiolite and palygorskite on heating. *American Mineralogist*, **53**, 1613–1624.
- Imai, N. and Otsuka, R. (1984) Sepiolite and palygorskite in Japan. Pp. 211–232 in: *Palygorskite-Sepiolite. Occurrences, Genesis and Uses*. (A. Singer and E. Galán editors). Developments in Sedimentology, **37**. Elsevier, Amsterdam.
- Jones, B.F. and Galán, E. (1991) Sepiolite and palygorskite. Pp. 631–674 in: *Hydrous Phyllosilicates (exclusive of micas)* (S.W. Bailey, editor). Reviews in Mineralogy, **19**. Mineralogical Society of America, Washington, D.C.
- Khorami, J. and Lemieux, A. (1989) Comparison of attapulgites from different sources using TG/DTG and FTIR. *Thermochimica Acta*, **138**, 97–105.
- Leguey, S., Pozo, M. and Medina, J.A. (1985) Polygenesis of sepiolite and palygorskite in a fluvio-lacustrine environment in the Neogene Basin of Madrid. *Mineralogica Petrographica Acta*, **29A**, 807–301.
- López Galindo, A., Ben Aboud, P., Fenoll Hach-Ali, P. and Casas Ruiz, J. (1996) Mineralogical and geochemical characterization of palygorskite from Gabasa (NE Spain). Evidence of a detrital precursor. *Clay Minerals*, **31**, 33–44.
- Martín Vivaldi, J.L. and Linares González, J. (1962) A random intergrowth of sepiolite and attapulgite. *Clays and Clay Minerals*, **9**, 592–602.
- McKeown, D.A., Post, J.E. and Etz, E.S. (2002) Vibrational analysis of palygorskite and sepiolite. *Clays and Clay Minerals*, **50**, 667–680.
- Mendelovici, E. (1973) Infrared study of attapulgite and HCl treated attapulgite. *Clays and Clay Minerals*, **21**, 115–119.
- Mifsud, A., Rautureau, M. and Fornes, V. (1978) Etude de l'eau dans la palygorskite à l'aide des analyses thermiques. *Clay Minerals*, **13**, 367–374.
- Newman, A.C.D. and Brown, G. (1987) Palygorskite and sepiolite. Pp. 107–112 in: *Chemistry of Clays and Clay Minerals* (A.C.D. Newman, editor). Monograph **6**, Mineralogical Society, London.
- Paquet, H., Duplay, J., Valleron-Blanc, M.M. and Millot, J. (1987) Octahedral compositions of individual particles in smectite-palygorskite and smectite-sepiolite assemblages. *Proceedings of the International Clay Conference, Denver*, pp. 73–77.
- Pozo, M., Medina, J.A. and Leguey, S. (1985) Mineralogénesis de paligorskita en la zona central de la Cuenca de Madrid. *Boletín Sociedad Española de Mineralogía*, 271–283.
- Post, R. (1973) Spectre infrarouge de l'eau présente dans l'attapulgite et la sepiolite. *Bulletin Française Argiles*, **XXV**, 53–63.
- Serna, C., Van Scyoc, G.E. and Ahlrichs, J.L. (1977) Hydroxyl groups and water in palygorskite. *American Mineralogist*, **62**, 784–792.
- Singer, A. and Norrish, K. (1974) Pedogenic palygorskite occurrences in Australia. *American Mineralogist*, **59**, 508–517.
- Suárez, M., Robert, M., Elsass, F. and Martín-Pozas, J.M. (1994) Evidence of a precursor in the neoformation of palygorskite – New data by analytical electron microscopy. *Clay Minerals*, **29**, 255–264.
- Suárez, M., Flores, L.V. and Martín Pozas, J.M. (1995) Mineralogical data for palygorskite from Bercimuel (Segovia, Spain). *Clay Minerals*, **30**, 261–266.

- Torres-Ruiz, J., López Galindo, A., González-López, J.M. and Delgado, A. (1994) Geochemistry of Spanish sepiolite-palygorskite deposits: Genetic considerations based on trace elements and isotopes. *Chemical Geology*, **112**, 221–245.
- Velde, B. (1985) *Clay Minerals. A Physico-Chemical Explanation of their Occurrence. Developments in Sedimentology*, **40**. Elsevier, Amsterdam.
- Verrecchia, E.P. and Le Coustumer, M.N. (1996) Occurrence and genesis of palygorskite and associated clay minerals in a Pleistocene calcrite complex, Sde Boqer, Negev Desert, Israel. *Clay Minerals*, **31**, 183–202.
- Vicente González, M.A., Suárez, M., Bañares, M.A. and López González, J. de D. (1996) Comparative FT-IR study of the removal of octahedral cations and structural modifications during acid treatment of several silicates. *Spectrochimica Acta (A)*, **52**, 1685–1694.
- Weaver, C.E. and Beck, K.C. (1977) Miocene of the S.E. United States; A Model for chemical sedimentation in a peri-marine environment. *Sedimentary Geology*, **17**, 234 pp.

(Received 20 November 2003; revised 3 March 2004;
Ms. 860)